Lateral Load Test of a Drilled Shaft in Clay

Harry M. Coyle and Richard E. Bartoskewitz, Department of Civil Engineering,
Texas Transportation Institute, Texas A&M University, College Station
Vernon R. Kasch*, McClelland Engineers, Inc., Houston, Texas

The behavior of a laterally loaded drilled shaft in clay was investigated by conducting a lateral load test on an instrumented shaft. Lateral deflections, shaft rotation, and soil resistance were measured for each applied load. Dial gages were used to measure lateral deflection, and the shaft rotation was determined by means of an inclinometer. Pneumatic pressure cells were installed in the shaft at various depths to measure the soil resistance. The applied lateral load was measured by using a strain-gage load cell. Structural failure of the shaft occurred before the soil failed and prevented determination of the ultimate lateral soil resistance. However, the ultimate soil reactions predicted by several analytical procedures were compared with the soil reaction calculated from the maximum recorded soil resistance. Also, an ultimate lateral load for the test shaft was predicted by various analytical methods, and a comparison was made between the maximum recorded load and the various predicted ultimate loads. Finally, a comparison was made between two ultimate test loads reported in the technical literature and the ultimate loads predicted by the analytical methods.

The Texas State Department of Highways and Public Transportation has in recent years developed a new concept in retaining-wall design and construction. The new type of retaining structure is the precast-panel retaining wall. As shown in Figure 1, this structure makes use of precast panels that are placed between T-shaped pilasters. The pilasters are spaced at even intervals and supported by drilled shafts (in other locales, these may be referred to as drilled piers, bored piles, or drilled caissons). The precast panel derives its restraining ability from the pilasters, which are located at the edges of the panel. The forces acting on the panel are transmitted to the pilasters and must be resisted by the soil in contact with the drilled shafts.

The drilled shaft must be designed to withstand both axial and lateral loads. However, because the axial load on a shaft supporting a precast-panel retaining wall is minimal, it is the lateral load that is of primary interest. Passive and active pressures are developed in the soil as a result of being in contact with the foundation. The magnitude and distribution of these pressures is dependent on many factors, including the size of the lateral load, the type of soil and its physical properties, and the diameter and flexibility of the foundation. Because the forces that resist lateral loads are the resultants of earth pressures, field pressure measurements should be beneficial in the development of improved design criteria.

Several investigators have made pressure measurements on cylindrical foundations. Stobie (1), in 1930, used mechanical pressure gages to measure soil pressures on laterally loaded utility poles. The pressures were calculated from the deformation of calibrated lead wires in the gages. Direct measurement of pressures on laterally loaded piles has been reported by Mason and Bishop (2) and by Heijnen and Lubking (3). Mason and Bishop used friction-steel, ribbon-type pressure gages, and Heijnen and Lubking used pressure cells, but did not specify the kind. Adams and Radhakrishna (4) report the use of hydraulic-displacement pressure cells on lateral-capacity tests of drilled shafts. In addition to these direct measurements of soil pressure, several other investigators have reported soil reactions that were determined indirectly from instrumented piles or drilled shafts (5-9). The soil reactions were determined by double differentiation of the bending moments that were obtained from strain-gage measurements.

Improvements in design procedures may result in significant savings in construction costs. The objective of this research study was to obtain field data by the measurement of loads, lateral earth pressures, deflections, and rotations on a laterally loaded drilled shaft. The results of the analysis of the field data will be used to develop rational criteria for the design of drilled shafts that support precast-panel retaining walls.

TEST SITE AND LOADING SYSTEM

A lateral load test was conducted on an instrumented drilled shaft to collect field data for use in the development of rational design criteria. To minimize potential installation problems with the shaft, a site consisting entirely of clay was selected. This site was found at the Texas A&M research annex at the southwest end of the northeast-southwest runway.

Soil conditions at the test site were investigated by using three soil borings and one Texas cone penetrometer (TCP) test. The boring locations, designated B-S1, B-S2, and B-S3, are shown in Figure 2. Undisturbed soil samples were taken with a 3.81-cm (1.50-in) thin-wall tube sampler. The location of the TCP test, designated TCP-1, is also shown in Figure 2.

Laboratory tests on the undisturbed samples included Atterberg limits, moisture contents, and unit weights. The undrained cohesive shear strength (C_u) of the samples was determined by unconfined compression tests and miniature vane tests. Typical results of the tests for boring B-S2 are shown in Figure 3. The test results indicated that the soil conditions were fairly uniform. The site consisted of stiff to very stiff clay having an average undrained cohesive shear strength of about 124 kPa (17.8 lbf/in^2). The clay to a depth of approximately 1.5 m (5 ft) had Unified Soil Classification of CL. The clay at a depth lower than approximately 1.5 m was classified as CH. A slickensided structure was noted in the clay at depths lower than about 3.0 m (10 ft).

The N-values (blow counts) obtained from the TCP test were also used to develop a shear-strength profile. The correlation developed by Duderstadt and others (10) was used to determine the undrained cohesive shear strength from the N-values. An average undrained cohesive shear strength of about 110 kPa (16 lbf/in^2) was obtained by using this method. This value compares quite well with the shear strength of 124 kPa obtained from the unconfined compression and miniature vane tests.

On completion of boring B-S3, an open standpipe was installed for groundwater observations. A perforated polyvinyl chloride pipe covered with screen wire was placed in the bore hole and surrounded with clean gravel. Water-level readings indicated that the water level was steady at a depth of 4.6 m (15 ft).

The loading and reaction system used in testing the instrumented drilled shaft is shown in Figure 4. The

reaction system consisted of two reinforced-concrete drilled shafts connected by a reinforced-concrete tie beam. Each shaft was drilled to a depth of 6.1 m (20 ft) and was 0.9 m (3 ft) in diameter. The shaft spacing was 6.1 m, center to center. The steel reinforcing cages for each shaft consisted of twelve no. 11 bars (grade 60) having a no. 3 spiral at a 15-cm (6-in) pitch. The beam connecting the shafts was approximately 1.2 m (4 ft) wide and 1.07 m (3.5 ft) deep. It was reinforced with 14 no. 6 steel bars having no. 3 stirrups at a 61-cm (24-in) spacing. A 5-cm (2-in) diameter steel reaction bar was embedded about 1.2 m deep on both reaction shafts. A steel plate was welded to each reaction bar to increase the bearing area. The winch was anchored to the rear reaction shaft by six 3.18-cm (1.25-in) anchor bolts embedded to a depth of approximately 1.2 m.

The test shaft was located on line with the centers of the reaction shafts at a center-to-center distance of approximately 9.1 m (30 ft) from the front reaction shaft. The shaft was nominally 0.9 m in diameter by 6.1 m deep. Wobble in the auger produced a diameter that varied from about 99 cm (39 in) at the ground surface to about 91 cm (36 in) at a depth of about 4.9 m (16 ft). The actual depth of the shaft was 6.16 m (20.2 ft). The reinforcing cage for the test shaft was the same as for the reaction shafts. As shown in Figure 4, the lateral load was applied to a steel column that was bolted to the test shaft. The column was a 12 WF 120, which was welded to a 2.5-cm (1-in) steel base plate. Twelve 3.18-cm anchor bolts were used to connect the column to the shaft. The bolts were embedded to a depth of 2.4 m (8 ft).

The lateral load was applied to the test shaft by a winch and pulley system. The winch was a single-drum, 178-kN [40 000-lbf (40-kip)] capacity Garwood cable winch driven through a four-to-one gear-reduction unit by a gasoline-powered hydraulic unit. A 12:1 mechanical advantage was provided by two, six-sheave, 890-kN [200 000-lbf (200-kip)] capacity pulley blocks. The cable was a 1.91-cm (0.75-in), 6x19 standard hoisting wire rope. As shown in Figure 4, one block was connected to the anchor bar and the other was connected to the test shaft. The load cell was placed between the block

Figure 1. Precast-panel retaining wall.

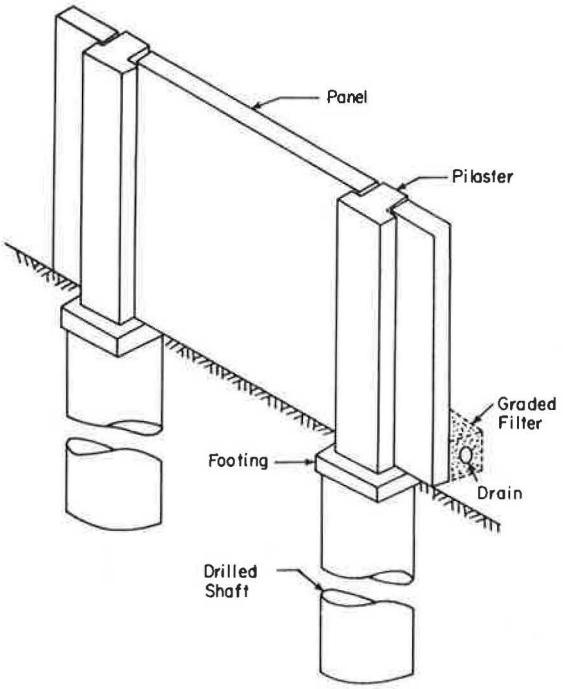

Figure 2. Location of borings.

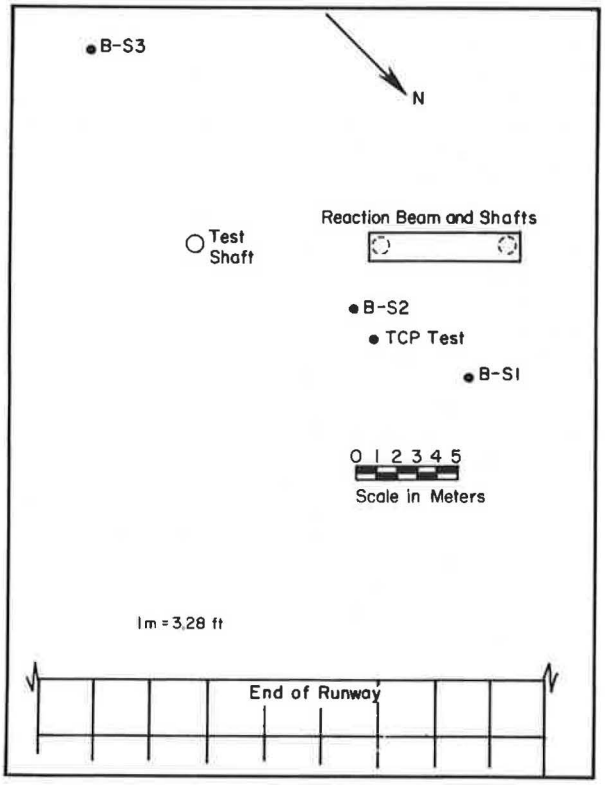

Figure 3. Boring log: B-S2.

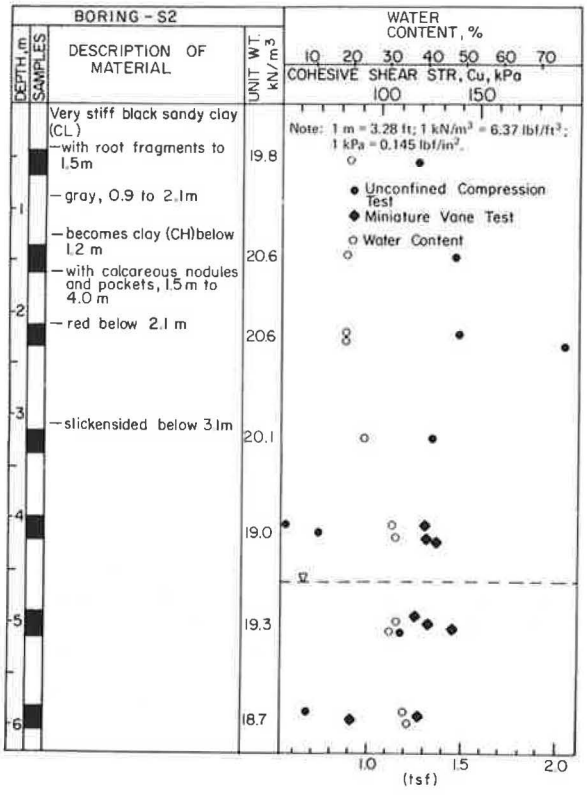

Figure 4. Lateral loading system.

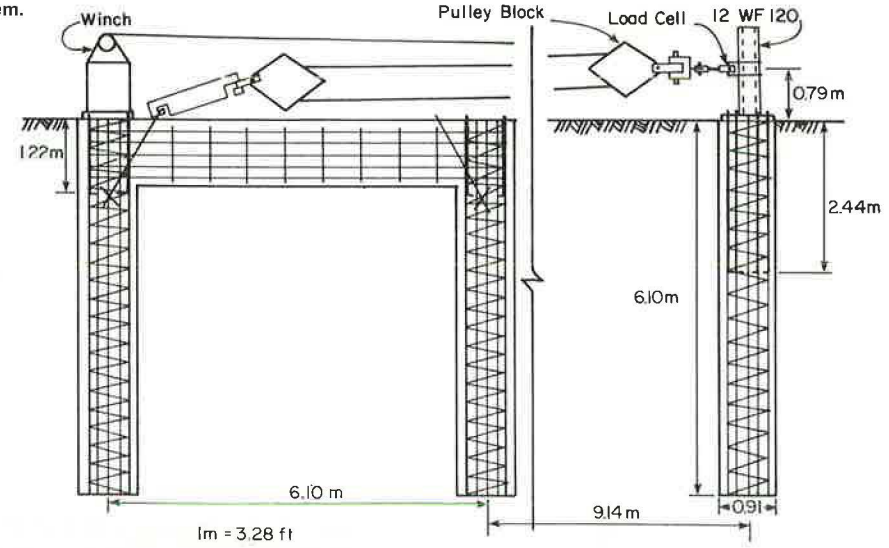

Figure 5. Location of pressure cells.

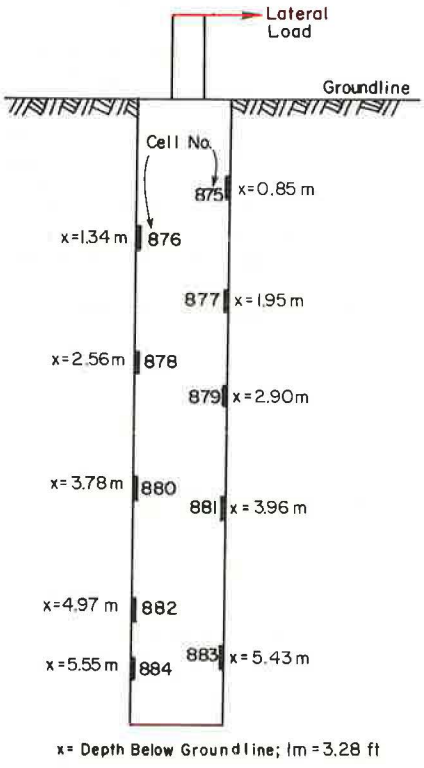

and the test shaft at a height of 0.79 m (2.6 ft) above the groundline.

INSTRUMENTATION AND LOADING PROCEDURE

The test shaft was instrumented with Terra Tec pneumatic pressure cells. These cells have been used successfully by Wright and others (11) in a study of active pressures on precast-panel retaining walls. Before the cells were installed in the test shaft, they were individually checked in a pressure chamber. The zero reading of each cell was determined; no malfunctions were observed in any of the cells.

The spacing and location of the pressure cells on the test shaft is shown in Figure 5. The cells were installed directly in line with the direction of the applied load. Five cells were located on the front of the shaft facing the reaction system, and five cells were located directly opposite on the back side. The cells were placed in the soil along the side of the excavation and held in place by steel pins.

The load applied to the test shaft was measured by a 890-kN-capacity strain-gage load cell. The load was indicated on a Budd P350 indicator in units of microstrain and converted from microstrain to kips by a predetermined calibration constant. The accuracy of the load cell and Budd indicator unit is approximately ±178 N (40 lbf).

The rotation of the shaft was determined by a Hilger and Watts TB108-1 inclinometer. The rotation could be read in degrees to an accuracy of approximately ±1 min. Rotational readings were taken by placing the inclinometer at five predetermined locations on the steel column. A back-up system was also devised for the determination of the shaft rotation. Horizontal measurements from a vertical reference line to five points on the steel column allowed the determination of the relative movements of the points. The reference line was established by using a plumb bob suspended from a frame welded to the top of the column. Initial measurements were made before the lateral load was applied and then subtracted from the subsequent measurements to obtain the movement relative to the initial position of the plumb line.

The deflection of the shaft at the groundline was measured by two 0.025-mm (0.001-in) dial gages. The gages were mounted on a steel beam behind the shaft, which was bolted to footings placed approximately 3.0 m (10 ft) on each side of the shaft. A bench mark was set about 15.2 m (50 ft) behind the shaft as a safety measure in case the dial gages were disturbed.

The decision to load test a drilled shaft having dimensions of 6.1-m depth and 0.9-m diameter was based on the study reported by Wright and others (11). The precast-panel retaining wall instrumented in that study was founded on drilled shafts having those dimensions. Because the lateral load acting on a drilled shaft supporting a precast-panel retaining wall is the resultant of the backfill acting on the panel, the initial loads applied to the test shaft were selected to simulate those loads.

Wright and others have presented a method for calculating the maximum resultant force of the backfill

Table 1. Initial pressure-cell readings.

Cell	Laboratory Zero Reading: April 1977 (kPa)	Shaft Initial Reading: May 24, 1977 (kPa)	Shaft Reading After Concrete Placement: May 24, 1977 (kPa)	Shaft Reading Before Application of First Load: June 23, 1977 (kPa)
875	63.5	51.1	60.1	51.1
876	114.5	113.7	128.3	113.2
877	53.1	49.7	67.6	59.3
878	48.3	44.9	57.3	44.9
879	69.0	62.1	78.7	71.8
880	69.0	52.4	62.1	55.2
881	72.5	69.0	85.6	79.4
882	104.9	97.3	116.6	119.4
883	53.1	45.5	71.1	72.5
884	79.4	74.5	103.5	106.3

Note: 1 kPa = 0.145 lbf/in^2.

Figure 6. Relationship between lateral pressure and depth.

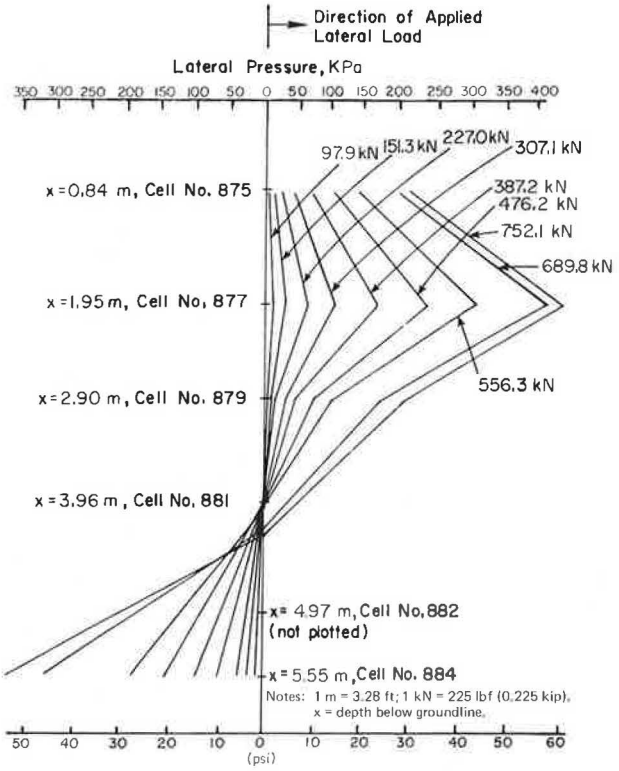

acting on a retaining wall. For the retaining wall reported in their study, the maximum resultant force was calculated to be 155 kN/shaft (34 900 lbf/shaft). The backfill producing the resultant force in that study was deposited over an eight-day period. To simulate the backfilling of that particular retaining wall as closely as possible, the initial loads on the test shaft in this study were applied over a six-day period. The applied force on the test shaft at the end of the six-day period was 153.5 kN [34 500 lbf (34.5 kips)]. Minor inaccuracies in the loading system prevented the exact simulation of the retaining-wall backfill.

After the load of 153.5 kN was applied, no additional loads were added for a period of 13 days in an attempt to determine whether any creep was occurring in the soil in front of the shaft. However, it was not possible to hold a constant load on the shaft, because daily temperature changes caused the cables in the loading system to expand and contract, creating a cyclic effect of as much as 31 kN/day (7000 lbf/day) in the applied load.

At the conclusion of the 13-day constant-load period, the load was increased daily in increments of approximately 40 kN [9000 lbf (9 kips)] until the lateral load reached 641 kN [144 000 lbf (144 kips)]. At that point, two steel pins connecting the load cell to the loading assembly and the shaft fractured. Consequently, the load had to be taken off the shaft and a two-week delay occurred while the connections were redesigned and rebuilt. When repairs were completed, the shaft was reloaded and the load test continued until structural failure of the shaft occurred at 752 kN [169 000 lbf (169 kips)]. Excavation of the shaft indicated that the reinforcing bars on the back of the shaft, along with the concrete, had fractured at a depth of 2.4 m (8 ft). The fracture occurred directly below the level of the anchor bolts.

TEST RESULTS AND ANALYSIS

Table 1 shows four sets of pressure cell readings: (a) the laboratory-calibration zero readings; (b) the initial readings taken after the cells were installed in the shaft, but before the concrete was placed; (c) readings taken after the concrete was placed; and (d) readings taken 30 days after concrete placement, but before the application of the first load.

As shown in Table 1, the initial zero readings taken in the shaft differed from the zero readings obtained in the laboratory calibration. In most cases, the readings taken in the shaft were 3.4-10.3 kPa (0.5-1.5 lbf/in^2) lower than the laboratory calibration; the reason for this is not known. As expected, the readings taken after the placement of the concrete were higher than the initial readings and the largest increases were recorded by the cells on the bottom of the shaft. Thirty days later, before the first lateral load was applied, cell readings indicated that most of the pressures had decreased by 7 kPa (1 lbf/in^2) or more, an effect that may be accounted for by concrete shrinkage during the 30-day curing period.

The lateral soil pressures resulting from the lateral loads on the shaft were determined by subtracting the initial cell readings from the cell readings obtained for a particular lateral load. The initial cell readings used were those obtained on June 23, just before application of the first lateral load. [Detailed pressure-cell data are described elsewhere (12).]

When the lateral pressures were calculated, the pressures recorded for cells 880 and 883 (see Figure 5) were consistently negative. It is probable that these two cells experienced a loss of contact with the soil as a result of rotation of the shaft, an effect that could have resulted in a pressure decrease. However, it should be noted that cells 876 and 878, which should also have experienced a loss of soil contact, did not record a significant number of negative pressures. This probably indicates that the initial pressures being used for cells

880 and 883 were too high by 7-14 kPa (1-2 lbf/in^2).

When the pressure cells were installed, it was assumed that the lateral loading would cause the shaft to rotate about a point 3.0-4.6 m (10-15 ft) deep. Consequently, the top three cells (see Figure 5) on the front side of the shaft (cells 875, 877, and 879) and the bottom two cells on the back side (cells 882 and 884) would be recording passive pressures and would have the highest pressure readings. These assumptions were essentially verified by the load test.

The pressure-cell data indicate that, of the five cells on the front side of the shaft, the top three (cells 875, 877, and 879) showed significant pressure increases and the fourth (cell 881) showed a slight increase. The pressure of the bottom cell (cell 883) was essentially constant. Of the five cells on the back side of the shaft, only the bottom one (cell 884) showed a significant increase in pressure. The pressures in the top three cells (cells 876, 878, and 880) remained constant, indicating essentially no active pressure, while the fourth cell (cell 882) showed a slight increase in pressure.

The lateral pressures indicated by cells 875, 877, 879, 881, and 884 are plotted with respect to depth for various lateral loads in Figure 6. The second cell from the top on the front side of the shaft (cell 877) consistently recorded the highest pressures. The next-highest pressures were recorded by the lowest cell on the back side (cell 884). The pressure recorded by cell 881 remained essentially constant; little or no lateral pressure was shown until the latter stages of the load test. This would seem to indicate that the rotation point of the shaft was in the general area of this pressure cell. The pressures recorded by cell 882 did not correlate well with those recorded by cell 884; cell 882 was located less than 0.6 m (2 ft) above cell 884 and yet did not record a lateral pressure in excess of 7 kPa until the load was more than 445 kN [100 000 lbf (100 kips)]. Because this cell was located in the slickensided clay, it is possible that some clay fell out from behind the cell during installation, thus creating an insufficient bearing area. Thus, the pressures recorded by cell 882 may be erroneous and, consequently, they are not included in Figure 6.

Considering the results shown in Figure 6, it is possible to draw some general conclusions about the shape of the lateral-soil-pressure distribution curve for cylindrical foundations in relatively homogeneous cohesive soil. (The lateral-soil-pressure distribution will be referred to as the soil resistance.) For loads that do not exceed the ultimate lateral resistance of the soil, the soil resistance appears to increase from some value in excess of zero at the ground surface to a maximum value that occurs at some depth between the ground surface and half of the foundation embedment and then decrease to zero at the rotation point (which occurs roughly between half and three-quarters of the foundation-embedment depth). Below the rotation point, the resistance again increases to a maximum value at the bottom of the foundation. It has been stated by Davisson and Prakash (13) that the upper point of maximum soil resistance shifts downward along the foundation, although the shape of the soil-resistance curve remains the same. The fixed location of the pressure cells on this test shaft prevented the observation of this phenomenon in this study.

As discussed above, the initial loads applied to the drilled shaft were a simulation of the loads produced during the backfilling of the retaining wall studied by Wright and others (11). The daily loads applied to the retaining wall, calculated from the data given by Wright and others, the loads applied to the test shaft, and the resulting deflections are shown below [1 kN = 225 lbf (0.225 kip) and 1 mm = 0.039 in].

Day	Calculated Load (kN)	Actual Load (kN)	Deflection (mm)
1	0.3		
2	2.4		
3	8.1	10.9	0.05
4	19.4	20.5	0.18
5	37.7	33.8	0.30
6	65.0	59.2	0.56
7	103.7	101.5	1.37
8	155.3	153.5	3.05
21	155.3	153.5	4.11

The table above also shows the deflection that occurred during the 13 days when no load was added to the shaft; the shaft movement during this period was only 1.07 mm (0.042 in). This movement was probably due to a combination of creep and a slight amount of structural breakdown of the soil due to the cyclic loading effect of the expanding and contracting cables caused by temperature variation.

The load-deflection curve for the load test is shown in Figure 7. The shaft had deflected 8.18 cm (3.22 in) when it failed structurally at 752 kN [169 000 lbf (169 kips)]. Figure 7 also shows the unloading and reloading curves that resulted from the two-week delay for repairs. It appears that the delay had little effect on the shape of the curve.

The load-rotation curve for the load test is shown in Figure 8. The structural failure of the shaft occurred at a rotation of about 2°. Laboratory tests conducted by Ivey and Dunlap (14) on model rigid piles indicate that the ultimate load for most of the tests occurred at a shaft rotation of about 5°. Figure 8 also indicates that there is a decrease in slope between the final portion of the initial loading curve and the initial portion of the reloading curve.

The location of the rotation point of the test shaft as indicated by the results of the inclinometer did not agree with the location indicated by the pressure cells. As the lateral load exceeded 445 kN, the inclinometer results (obtained by dividing the measured deflection of the shaft at the ground surface by the tangent of the rotation angle) indicated that the shaft was rotating about a point approximately 2.4 m (8 ft) deep. The pressure-cell readings seemed to indicate that the rotation point was in the area of cell 881, i.e., about 4.0 m (13 ft) deep. After the structural failure of the shaft, it became apparent that flexural bending had been occurring below the bottom of the anchor bolts at a 2.4-m (8-ft) depth. Consequently, the shaft was probably rotating as a unit about a point approximately 4.0 m deep and, at the same time, experiencing a flexural rotation at a depth of 2.4 m (8 ft).

Analytical studies by Hays and others (15) indicate that the rotation point is not constant but shifts downward from some point below the middle of the foundation for light loads to a point beyond three-quarters of the embedment depth for failure loads. Because the test shaft in this study experienced flexural bending and an ultimate load was not attained, it was not possible to verify Hays' results.

ULTIMATE SOIL RESISTANCE

Because structural failure occurred in the test shaft before soil failure was attained, it was not possible to determine the ultimate lateral soil resistance. However, it is possible to compare the soil resistance recorded by the pressure cells for the highest applied lateral load with the calculated ultimate soil reactions predicted by others. The soil reaction (p) is defined as the force per unit length of shaft. It can be calculated by multiplying the soil resistance by the shaft diameter (B). Figure 9 presents a comparison of the soil reactions to a depth of 3.0 m (10 ft) recorded on the test

Figure 7. Relationship between lateral load and deflection at groundline.

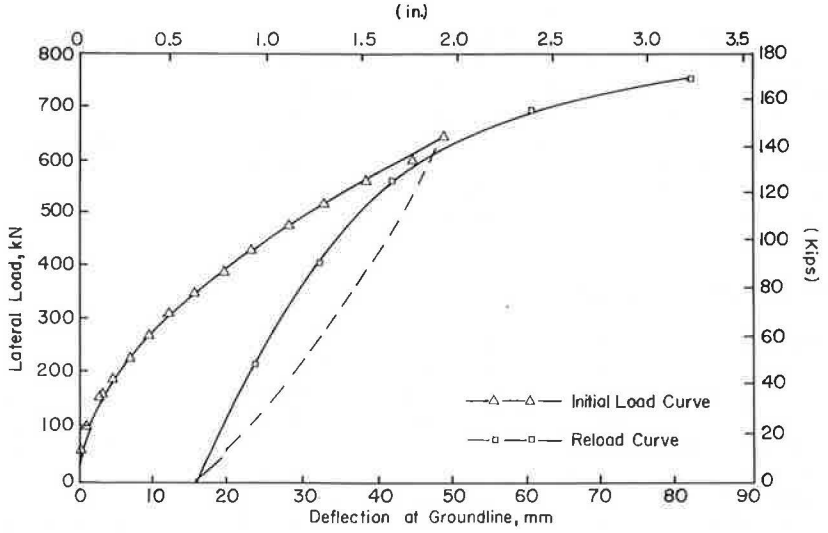

Figure 8. Relationship between lateral load and rotation.

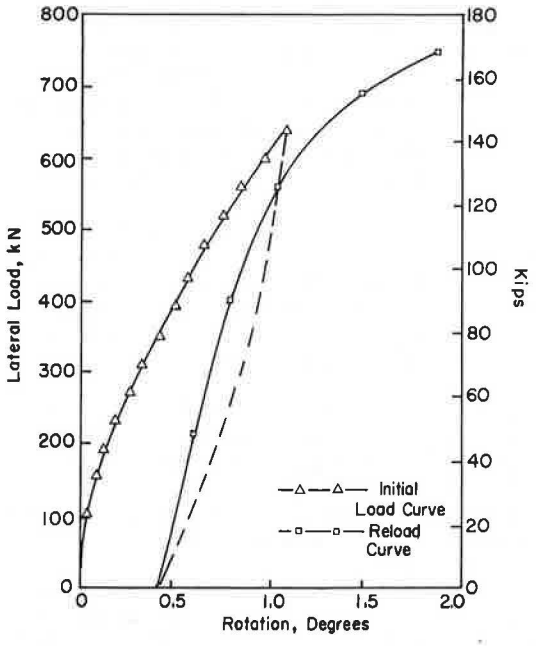

Figure 9. Relationship between ultimate soil reaction and depth below groundline.

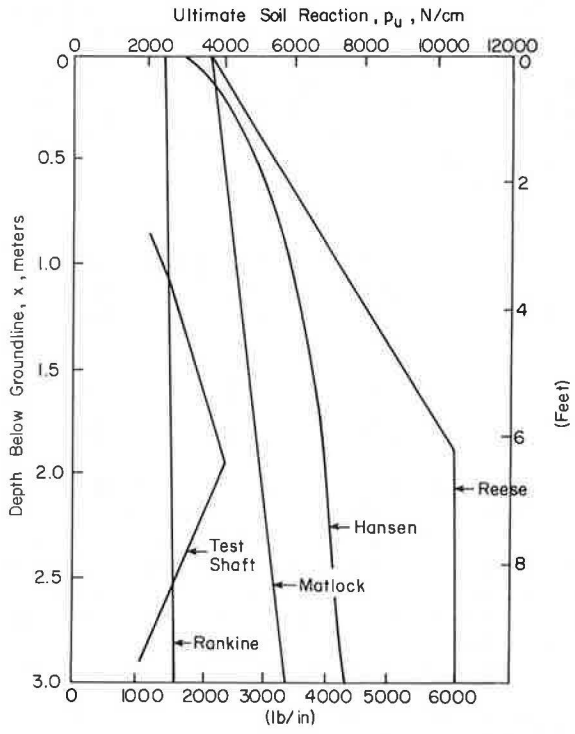

shaft at the maximum load of 752 kN [169 000 lbf (169 kips)] with the ultimate soil reactions (p_u) calculated by the methods proposed by Rankine (16), Hansen (17), Matlock (6), and Reese (18). The soil reaction for the test shaft was calculated from the pressures recorded on cells 875, 877, and 879. The following equations were used to predict the ultimate soil reactions:

Rankine

$$p_u = (\gamma x + 2C_u) B \quad (1)$$

Hansen

$$p_u = K_c C_u B \quad (2)$$

Matlock

$$p_u = [3 + (\gamma x/C_u) + (0.5x/B)] C_u B \quad (3)$$

and

Reese

$$p_u = [3 + (\gamma x/C_u) + (2.83x/B)] C_u B \quad (4)$$

where

γ = unit weight of the overburden material,
C_u = undrained shear strength of the soil,
x = depth below the ground surface, and
K_o = calculated earth-pressure coefficient.

Figure 9 indicates that, even though the load test did not produce ultimate soil reactions, the Rankine predictions were exceeded, thus verifying the conservative nature of this method. The equation used by Matlock, which is based on Reese's general equation, has been

empirically adjusted by using the results of lateral load test on piles in soft clays. However, in lateral load tests in stiff clays, Matlock's equation has in some instances predicted satisfactory results, while Reese's equation has given values in excess of those determined experimentally (8, 9). Additional testing will be needed before it can be determined which of the above equations can best predict ultimate soil reactions. This is especially true because an ultimate value was not attained on this test.

ULTIMATE LATERAL LOADS

The phrase "ultimate lateral load" as used in this paper means the maximum lateral load that the soil in contact with the foundation can withstand. Continued foundation deflection and rotation may occur with no increase in load when the ultimate load is reached. Many methods for calculating the ultimate load of a foundation can be found in the literature. Among these are the methods of Ivey and various coworkers (14, 18-21), Seiler (22), Hays and others (15), Broms (23), and Hansen (17). In addition, Ivey and Dunlap (20) have presented data from full-scale field tests of rigid shafts conducted at Bryan, Texas, and Galveston, Texas. Although an ultimate load was not attained for the load test described in this paper, it is informative to compare the predicted ultimate loads calculated by the aforementioned methods with the highest load applied to the test shaft. The table below presents a comparison of calculated ultimate loads and the measured loads for the load test described in this paper and for the two field tests reported by Ivey and Dunlap [1 kN = 225 lbf (0.225 kip)].

	Load (kN)		
Method	Current Study	Galveston Test	Bryan Test
Measured	752.1	24.5	55.2
Ivey and Dunlap	1272.7	12.8	67.4
Ivey and Dunlap with $\phi = 0$	578.5	6.0	38.8
Ivey and Hawkins	396.1	4.3	26.4
Broms	1157.0	6.9	42.5
Hays and others	983.5	7.8	39.8
Hansen	1206.0	9.0	55.2

Of the three load tests, the Bryan test probably offers the best comparison. The Galveston test was conducted without any problems but, as shown above, the measured load greatly exceeded any of the predicted ultimate loads. This was probably due to a stiff surface layer of clay that had a cohesive shear strength six times greater than the shear strength of the soil on the lower half of the shaft. It should also be noted that two variations of the method given by Ivey and Dunlap were used to calculate ultimate loads. This method is a semiempirical one in which a modifying factor is applied to the Rankine coefficients of passive and active earth pressure. Laboratory tests on cohesive samples to determine the modifying factor for these types of soils were conducted in such a way that both the angle of shearing resistance (ϕ) and the undrained cohesive shear strength (C_u) were determined. Consequently, the determined modifying factor assumes the use of both the cohesive shear strength and the angle of shearing resistance when determining the ultimate load of a foundation.

As expected, the Ivey and Hawkins method, which is based on Rankine passive earth pressures, consistently gives the most conservative results. The Ivey and Dunlap method with $\phi = 0$ also gives consistently conservative results, although not nearly as conservative as those of the Ivey and Hawkins method. The Ivey and Hawkins method underpredicted the measured load for the Galveston test by 473 percent, while the Ivey and Dunlap method was conservative by 307 percent. For the Bryan test, the Ivey and Hawkins method was 108 percent on the conservative side, while the Ivey and Dunlap method was conservative by 42 percent. The Ivey and Dunlap method, using both the cohesive shear strength and the angle of shearing resistance, consistently predicted the highest ultimate load. The method was conservative by 91 percent for the Galveston test, but 18 percent unconservative for the Bryan test. The other three methods—Broms, Hays and others, and Hansen—all predicted ultimate loads between those predicted by the two variations of the Ivey and Dunlap method.

CONCLUSIONS

Even though the test shaft failed structurally during lateral loading and an ultimate load was not attained, several useful observations were made during the test.

1. The serviceability and aesthetic appeal of a retaining wall depend on the amount of lateral deflection experienced by the wall. However, the magnitude of deflection that may be allowed is arbitrary. When the resultant force corresponding to that measured on the wall reported by Wright and others (11) was applied to the test shaft, the magnitudes of the resulting deflection, rotation, and soil reaction were small. Based on these observations, it is concluded that the drilled shafts supporting the precast retaining wall studied by Wright and others were probably overdesigned. Probably, the dimensions of those shafts could have been reduced by some amount without resulting in an objectionable deflection.
2. Before the structural failure of the test shaft occurred, its lateral deflection was of such magnitude as to probably be aesthetically objectionable. It is concluded that allowable deflection, rather than ultimate lateral load, may be the controlling criterion for the design of drilled shafts supporting precast-panel retaining walls.
3. The Ivey and Hawkins design method, which is based on Rankine's passive-earth-pressure formula, is not recommended for the design of laterally loaded drilled shafts because of its conservative nature. As shown by Figure 9, even though the lateral load test did not produce ultimate soil reactions, the Rankine predictions were still exceeded.
4. Based on the comparison of the load tests shown above, it is concluded that the Ivey and Dunlap method with $\phi = 0$ will produce conservative designs for drilled shafts. However, its use is recommended until additional lateral load tests can be conducted.

ACKNOWLEDGMENT

We gratefully acknowledge the support and assistance of the Texas Department of Highways and Public Transportation and the Federal Highway Administration, U.S. Department of Transportation, for their cooperative sponsorship in making this study possible.

The contents of this paper reflect our views; we are responsible for the facts and accuracy of the data presented herein. The contents do not necessarily reflect the views or policies of the Federal Highway Administration. This paper does not constitute a standard, specification, or regulation.

REFERENCES

1. J. C. Stobie. Pole Footings. Journal of the Institute of Engineers, Australia, Vol. 2, 1930, pp. 58-63.

2. H. G. Mason and J. A. Bishop. Measurement of Earth Pressure and Deflection Along the Embedded Portion of a 40-ft Steel Pile. ASTM, Special Tech. Publ. 154-A, 1954, pp. 1-21.
3. W. J. Heijnen and P. Lubking. Lateral Soil Pressure and Negative Friction on Piles. Proc., 8th International Conference on Soil Mechanics and Foundation Engineering, Moscow, USSR, Vol. 2.1, 1973, pp. 143-147.
4. J. I. Adams and H. S. Radhakrishna. The Lateral Capacity of Deep Augered Footings. Proc., 8th International Conference on Soil Mechanics and Foundation Engineering, Moscow, USSR, Vol. 2.1, 1973, pp. 1-8.
5. B. McClelland and J. A. Focht, Jr. Soil Modulus for Laterally Loaded Piles. Journal of the Soil Mechanics and Foundations Division, Proc., ASCE, Vol. 82, No. SM4, Oct. 1956, pp. 1081-1 to 1081-22.
6. H. Matlock. Correlations for Design of Laterally Loaded Piles in Soft Clay. Proc., 2nd Annual Offshore Technology Conference, Houston, TX, May 1970, pp. 577-594 (paper OTC 1204).
7. L. C. Reese, W. R. Cox, and F. D. Koop. Analysis of Laterally Loaded Piles in Sand. Proc., 6th Annual Offshore Technology Conference, Houston, TX, May 1974, pp. 473-483 (paper OTC 2080).
8. L. C. Reese, W. R. Cox, and F. D. Koop. Field Testing and Analysis of Laterally Loaded Piles in Stiff Clay. Proc., 7th Annual Offshore Technology Conference, Houston, TX, May 1975, Vol. 2, pp. 671-690 (paper OTC 2312).
9. R. C. Welch and L. C. Reese. Lateral Load Behavior of Drilled Shafts. Center for Highway Research, Univ. of Texas at Austin, Res. Rept. 89-10, May 1972.
10. F. J. Duderstadt, H. M. Coyle, and R. E. Bartoskewitz. Correlation of the Texas Cone Penetrometer Test N-Value with Soil Shear Strength. Texas Transportation Institute, Texas A&M Univ., College Station, Res. Rept. 10-3F, Aug. 1977.
11. W. V. Wright, H. M. Coyle, R. E. Bartoskewitz, and L. J. Milberger. New Retaining Wall Design Criteria Based on Lateral Earth Pressure Measurements. Texas Transportation Institute, Texas A&M Univ., College Station, Res. Rept. 169-4F, Aug. 1975.
12. V. E. Kasch, H. M. Coyle, R. E. Bartoskewitz, and W. G. Sarver. Lateral Load Test of a Drilled Shaft in Clay. Texas Transportation Institute, Texas A&M Univ., College Station, Res. Rept. 211-1, Nov. 1977.
13. M. T. Davisson and S. Prakash. Review of Soil-Pole Behavior. HRB, Highway Research Record 39, 1963, pp. 25-48.
14. D. L. Ivey, K. J. Koch, and C. F. Raba, Jr. Resistance of a Drilled Shaft Footing to Overturning Loads: Model Tests and Correlation with Theory. Texas Transportation Institute, Texas A&M Univ., College Station, Res. Rept. 105-2, July 1968.
15. C. O. Hays, J. L. Davidson, E. M. Hagan, and R. R. Risitano. Drilled Shaft Foundation for Highway Sign Structures. Engineering and Industrial Experiment Station, Univ. of Florida, Gainesville, Res. Rept. D647F, Dec. 1974.
16. K. Terzaghi and R. B. Peck. Soil Mechanics in Engineering Practice, 2nd ed. Wiley, New York, 1967, pp. 198-200.
17. J. B. Hansen. The Ultimate Resistance of Rigid Piles Against Transversal Forces. Danish Geotechnical Institute, Copenhagen, Bull. 12, 1961.
18. L. C. Reese. Discussion of paper, Soil Modulus for Laterally Loaded Piles, by B. McClelland and J. A. Focht, Jr. Trans., ASCE, Vol. 124, 1958, pp. 1071-1074.
19. D. L. Ivey. Theory, Resistance of a Drilled Shaft Footing to Overturning Loads. Texas Transportation Institute, Texas A&M Univ., College Station, Res. Rept. 105-1, Feb. 1968.
20. D. L. Ivey and W. A. Dunlap. Design Procedure Compared to Full-Scale Tests of Drilled Shaft Footings. Texas Transportation Institute, Texas A&M Univ., College Station, Res. Rept. 105-3, Feb. 1970.
21. D. L. Ivey and L. Hawkins. Signboard Footings to Resist Wind Loads. Civil Engineering, Vol. 36, No. 12, Dec. 1966, pp. 34-35.
22. J. F. Seiler. Effect of Depth of Embedment on Pole Stability. Wood Preserving News, Vol. 10, No. 11, Nov. 1932, pp. 152-168.
23. B. B. Broms. Lateral Resistance of Piles in Cohesive Soils. Journal of the Soil Mechanics and Foundation Division, Proc., ASCE, Vol. 90, No. SM2, March 1964, pp. 27-63.

Publication of this paper sponsored by Committee on Foundations of Bridges and Other Structures.

**V. R. Kasch was at the Texas Transportation Institute when this research was performed.*

Geology and Tunneling Economics in Montreal

Hugh Grice, Department of Geological Sciences, McGill University, Montreal
Marc Durand, Department of Earth Sciences, Université du Québec à Montréal

The economic construction of transportation projects depends in part on the availability of all relevant geological and geotechnical data. In Montreal, Canada, all of the 120 km (75 miles) of subways, major sewers, and aqueducts constructed during the last 18 years have been affected by local geological factors. Contracted costs for subway tunnels in shale were about 20 percent higher than for those in limestone. Locally, the presence of weathered zones in limestones and shales, where they have been faulted or intruded, increased actual costs to six times the normal unit price in good limestone. The contracted cost was 12.5 times the normal for a transition from an open cut into a tunnel in soil or rock. Variations of costs for contractors were estimated from rates of advance, amounts of concrete required to backfill overbreaks, and numbers of